EXPERIMNTAL STUDY ON Sn-Bi-In MELT-SPUN RIBBONS FOR INTERMEDIATE-STEP SOLDERING

*Mustafa Kamal , Abu-Bakr El-Bediwi ,Shalabia Badr , and Sabah Taha**

Metal Physics Lab. Physics Department, Faculty of Science –Mansoura University, Egypt.

**on leave, M.sc student, Ministry of Higher Education, Yemen.*

kamal422002@yahoo.com , baker_elbediwi@yahoo.com ,

sabahtaha96@yahoo.com

Abstract— ***we chose Sn10Bi, Sn10Bi10In, Sn20Bi, and Sn20Bi20In (numbers are in weight percent) rapidly solidified from melt using melt-spinning technique for intermediate –step soldering. We then investigated the structure, electrical and mechanical properties of the melt-spun ribbons using x-ray diffraction, double bridge circuit, dynamic resonance technique, and Vickers microhardeness tester. It was concluded that Sn10Bi10In as Pb-Free solder for intermediate-step soldering is the best solder in micromechanical system packaging as a hermetic sealing step.***

Keywords—Melt-spin technique, SnBiIn, structure, Electrical, Mechanical properties, and Step Soldering

I. INTRODUCTION

There has been considerable scientific and technological Interest in using rapid solidification processing, with cooling rates during solidification of $>10^5$ ks^{-1} to produce new structures and improved properties in a variety of metallic alloys. The tin-bismuth –indium system has attracted attention in recent times because it has potential application in microelectronic mechanical system packaging [1-4]. Sun-Kyoung Seo et al [5] have conducted systematic experiments on the formation mechanism of the intermetallic phases of the Sn-2.8wt%Ag-20wt%In and Sn-10wt%Bi-10wt%In as Pb-free solder materials for intermediate-step soldering. On the basis of their observations, they prefer the Sn2.8Ag20In solder to Sn10Bi10In solder for intermediate-step soldering because the Sn2.8Ag20In solder has a smaller number of intermetallic compound phases as well as a slower intermetallic compound growth rate and higher shear strength. So their results indicated that the SnBiIn joint has weaker shear strength than the SnAgIn solder joint

II. Scope of this Research

The goal of the present study is to explore the effect of rapid solidification from melt on the properties of SnBiIn solder for intermediate –step soldering. This is followed by a detailed study on the structure, electrical, and mechanical behavior of the Sn10Bi, Sn20Bi, Sn10Bi10In and Sn20Bi20In (numbers are in weight percent) melt-spun ribbons as Pb-free solder alloys in the microelectronic industry.

III. MATERIAL AND METHODS

The material used in the present work are, Sn, Bi, and In fragments the starting purity was better than 99.99%. A group of Sn10Bi,Sn10Bi10In, Sn20Bi,and Sn20Bi20In melt-spun alloys (composition are all in weight percent) were produce by single copper roller (200mm in melt-diameter)spinning technique[6].The process parameters Such as the ejection temperature, and the linear speed of the wheel were fixed at 550k and 30.4ms^{-1} respectively. Resulting melt spun alloys had long ribbon forms of about 50μm thick and about 1cm in width. Estimated cooling rates were $10^5 ks^{-1}$. The structure of these melt-spun alloys was examined by the x-ray diffraction (XRD) technique (DX-30), using cukα radiation (λ=1.5406Å) with Ni-filter. Electrical resistivity values and the temperature dependence of resistivity values were calculated using double –bridge circuit with heating rate 5k min^{-1}. The detail of the double bridge method was described elsewhere [7]. The values of dynamic young's modulus E, and the internal friction Q^{-1} were calculated using the dynamic resonance from the following relationship [8, 9]:

$$E = 38.32\frac{\rho L^4 f^2}{t^2} \quad (1)$$

$$Q^{-1} = 0.5773\frac{\Delta f}{f} \quad (2)$$

Where ρ the density of the sample test, L is the length of the vibrated of the melt-spun ribbon, f is the resonance frequency of the sample and t is the sample's thickness. In particular, shear modulus, G and bulk modulus, B may be estimated from the young's modulus, E and Poisson's ratio, σ,:

$$B = \frac{E}{3(1-2\sigma)} \quad (3)$$

$$G = \frac{E}{2(1+\sigma)} \quad (4)$$

For many Sn-Bi alloys, Poisson's ratio is

approximately 0.33. Learning about the anelastic behavior of SnBiIn melt-spun ribbons has been quite fruitful. It has been found that anelasticity is very sensitive [10, 11] to small changes in the mechanical state of a material, it can be used to study the effects of various treatments. Also, anelastic relaxation can be used to measure conveniently some properties such as thermal diffusivity from the frequency $_f$, at which the peak damping occurs, the thermal diffusivity D, can be obtained directly from the relation:

$$D = \frac{2t^2 f}{\pi} \qquad (5)$$

Hardness measurements were carried out using the Vickers micro-hardness tester. Fifteen measurements were taken for each melt-spun ribbon using a load of 10 grams of force for 5 seconds.

IV. RESULT AND DISCUSSIONS

Structural analysis

The XRD patterns shown in (fig1) are obtained from the middle of the ribbons (a) pure Sn,(b)Sn10Bi,(c) Sn10Bi10in,Sn20Bi2oIn,(d)Sn20Bi,and (e) Sn20Bi20In the as-rapidly solidified from melt respectively. It is clear that the prominent peaks occurring in the XRD pattern in the SnBi and SnBiIn melt-spun ribbons contain all the peaks shown in XRD patterns attributed to the phases of tin and bismuth. But in the case of ternary melt-spun SnBiIn has a diffraction lines of β -Sn phase and Bi-phase while only a few very weak (112), and (200) reflections, can be recognized for tetragonal indium phase. In addition, no other peaks that might be attributed to metal oxides were found in pattern, which indicated that no oxidation reactions took place in the process. From the above discussion it can be concluded that the SnBiIn rapidly solidified from melt are the ternary solder alloy, which consists of the tetragonal phase of tin, the rhombohedra phase of bismuth and a very weak reflections from indium tetragonal phase. This effect was interpreted as indication that the solidification rate for SnBiIn ribbons was high enough to retain most of the alloying elements in solid solution. To determine the amount of retained indium upon rapid quenching, the cell parameters of β -Sn phase are presented in table (1)

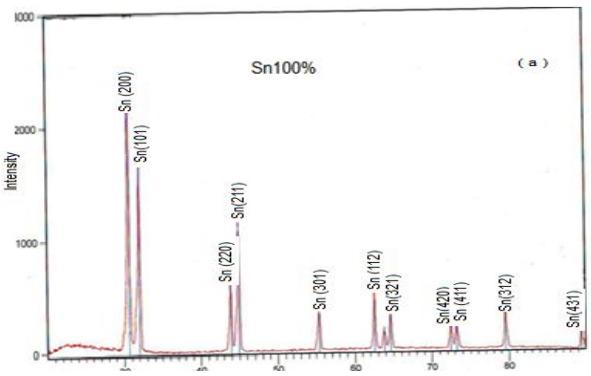

$2\theta(\deg ree)$

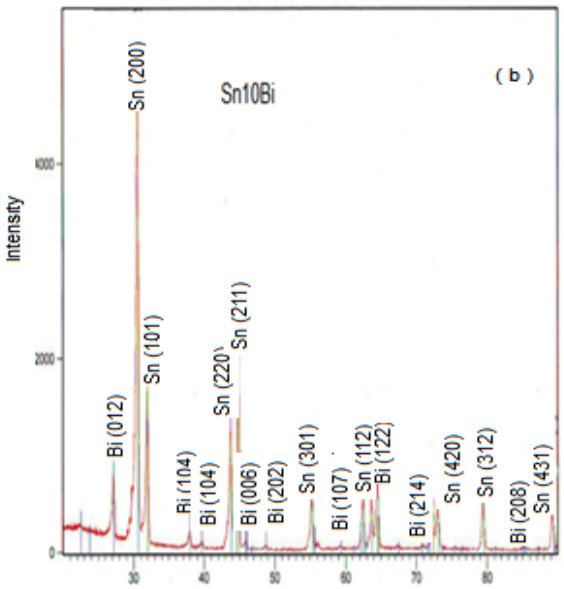

$2\theta(\deg ree)$

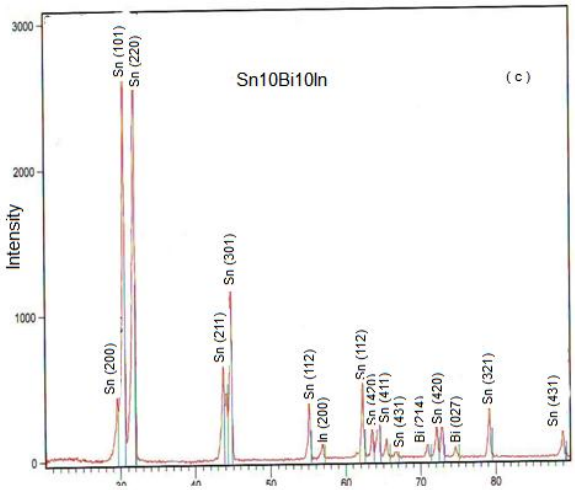

$2\theta(\deg ree)$

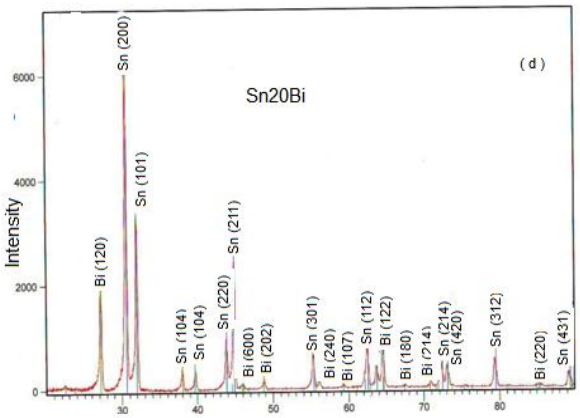

$2\theta(\deg ree)$

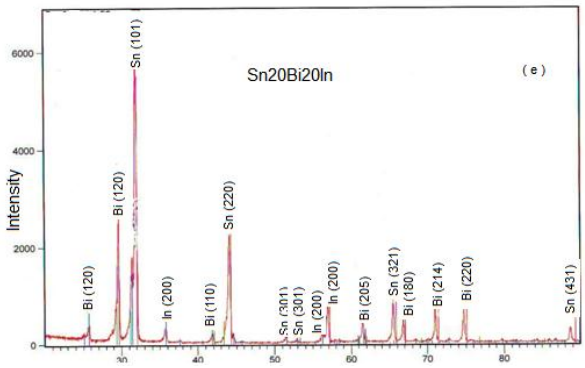

Figure (1, a, b, c, d and e)

System	a (Å)	c (Å)	c/a	Cell volume(Å^3)
Sn100%	5.85	3.192	0.546	109.024
90Sn10Bi%	5.85	3.184	0.544	109.0625
80Sn20Bi%	5.85	3.186	0.545	108.9956
80Sn10Bi10In%	6.84	3.131	0.458	146.438
60Sn20Bi20In%	5.79	4.48	0.773	150.484

Table (1) cell parameters

These values imply different shifts in the lattice constants of β-Sn for different compositions. Theoretically the lattice parameter of β-Sn decreases with In content in solid solution and the size of the decreases has been suggested to be related to the closest distance constituent atoms. In the case of Sn20Bi20In and Sn10Bi10In melt-spun ribbons, it is found that the tetragonal cell of tin-rich-phase is low stretched with a=6.83Å, and c=3.1309Å for Sn10Bi10In but in the case of Sn20Bi20In with a=5.797Å and c=4.478Å, as shown in table (1) with a cell volume in the range of 146.44 to 150.49Å^3. The result of this is to add more lines to the pattern. The a and c parameters of the tin-rich –phase cell differs greatly from the cell of the tin-phase in Sn10Bi or Sn20Bi melt-spun alloys. It is reported that the cell of Sn-phase in SnBiIn tend to decrease the amount of distortion. The changes produced in the melt-spun ribbons diffraction pattern by cell distortion, depend, in degree, on the amount of distortion. If the latter is small, the pattern retains the main feature of the pattern of the original undistorted cell.

V. Number of atoms in a unit cell

The next step after indentifying the phases is to find the number of atoms in the β-Sn-rich-phase in each melt-spun ribbons of the system used in this study. So we have the following equation [12].

$$\sum A = \frac{\rho v}{1.66020} \quad , \qquad (6)$$

$$\sum A = nM$$

Where $\sum A$ is the sum of the atomic weights of the atoms in the unit cell, ρ is the density (gm/cm^3), and v is the volume of the unit cell. The number of atoms per cell can then calculated from n and the composition of the phase, and M is the molecular weight. When determined in this way, the number of atoms per cell is always an integer, within experimental errors, except for a very few melt-spun ribbons which have defect structures. In these melt-spun ribbons as showed in table (2), atoms are simply missing from a certain fraction of those lattice sites, which they would be expected to occupy, and the result is a nonintegral number of atoms per cell.

System	Number of atoms per unit cell
Sn	4
Sn10Bi	2.6
Sn10Bi10In	5.04
Sn20Bi	3.3
Sn20Bi20In	3.92

Table (2)

VI. RESISTIVITY

Anything which increases the frequency of collisions of electrons with ions raises the resistivity, Thermal vibration, foreign atoms in solid solution, and plastic deformation of the lattice lower the conductivity. Thus it is found in this study that the electrical resistivity of the studied melt-spun alloys increase with rise in temperature as indicated in figures (2, a ,b) for Sn10Bi, Sn10Bi10In, Sn20Bi and Sn20Bi20In.

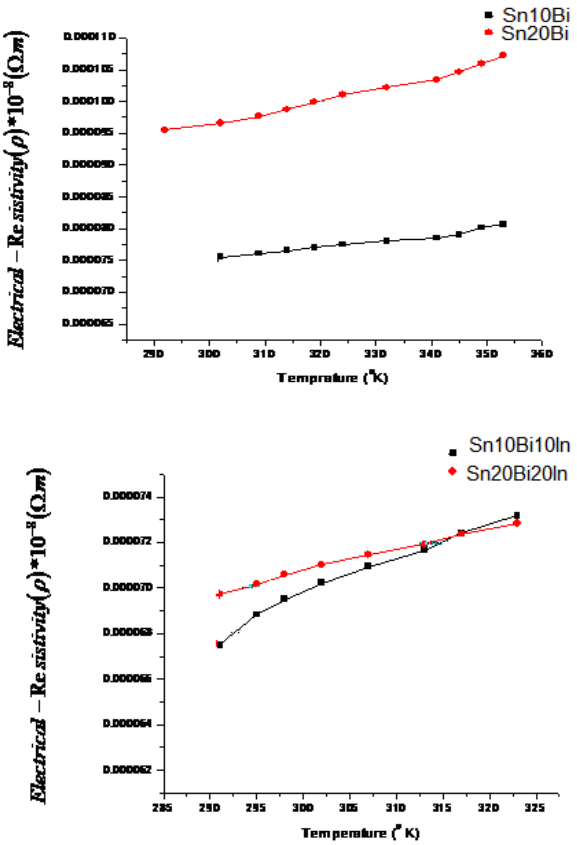

Figure (2, a, b)

The distortions produced by alloying elements are independent of the temperature. Their effects are additive to the effect of thermal vibration. At higher temperatures the thermal disturbance of the lattice can be described in terms of quantized elastic waves or phonons, and the increase in electrical resistivity can be visualized as resulting from collisions between electrons and phonons. It is found that the resistivity of pure Sn rapidly solidified is increased with the addition of bismuth up to $95.52x10^{-8}\Omega m$. due to high concentration of vacancies in the matrix, which hinder the motion of conduction electrons from one site to another in the matrix. In the case of the melt-spun ribbons of SnBiIn, the resistivity falls down to the value $63x10^{-8}\Omega$m.It is clarified that when the indium content added to SnBi a decrease in resistivity occurs because of the disruption of the orderly atomic arrangement is removed during the solidification of SnBiIn, So a net increase in the conductivity occurs. The grain –refining effects of the In addition reported herein are most likely the result of an increased number of nucleation sites upon solidification and/or possible slow growth kinetics due to In. It has been found that additions about 10 to 20wt% indium in SnBi solder alloys improve the electrical conductivity. The improvement in conductivity can be brought about by reduced scattering conduction electrons also. The smooth reduction in conduction electrons scattering can result due to thermally activated nucleation and subsequent diffusion controlled growth.

VII. THERMAL DIFFUSIVITY

Thermal diffusivity, D is transport coefficient which is related to microscopic transport of heat. This value is directly associated with a change of temperature of material. It is noted from table (3) that the thermal diffusivity of the melt.-spun ribbons used in this work is a non-linear increase or decrease of thermal diffusivities with or without indium contend observed in all case. The thermal diffusivity of Sn20Bi20In is higher than thermal diffusivity of Sn10Bi10In, So the thermal diffusivity in this case is a function of In content or the composition. Since thermal diffusivity of all types of the melt-spun ribbons is different, we assume that this fact is caused by rapid solidification process. So this technique could improve a heat transport in the materials and improve thermal diffusivity, particularly in the case of Sn20Bi20In melt-spun ribbons.

System	$D_{th}x10^{-8}\left(m^{2.}.\sec^{-1}\right)$
Sn	2.489
Sn10Bi	30.968
Sn10Bi10In	9.90166
Sn20Bi	15.367
Sn20Bi20In	82.6124

Table (3)

VIII. ELASTIC PROPERTIES OF QUENCHED PRODUCTS

Elastic materials have characteristic set of natural acoustical resonance frequencies, which are determined by the elastic moduli, the specific density, and the dimensions of the ribbons used in this study. Thus it is evident to use these frequencies as a tool to determine the elastic moduli. A number of researches have given the empirical relationships to relate shear nodulus (G), bulk modulus (B), and the young's modulus (E) for various elements [13-15] by the equations (3, 4). The Poisson's ratio for melt-spun alloys used in this contribution were about 0.33. table (4) shows young's modulus, shear modulus, and bulk modulus. It should be pointed out that the measurement of the elastic moduli is quite complicated for highly sensitive microstructrally evolving and highly sensitive, volume fraction of precipitates, and may be sensitive to electron concentration[16] The unit-cell volume of β-Sn-rich-phase for all the melt-spun ribbons studied is indicated in table (4).

System	E (GPa)	B (GPa)	μ (GPa)	Cell volume(Å^3)
Sn	33	32	12	109.024
Sn10Bi	39	39	15	109.063
Sn10Bi10In	38	37	14	146.438
Sn20Bi	34	33	13	108.996
Sn20Bi20In	23	23	8	150.484

Table (4)

It can be seen that the unit cell volume is expanded with the addition of indium content was particularly noticed in the Sn20Bi20In melt-spun ribbons. This means that the increased unit-cell volume lead to decrease the elastic modulus of the studied alloys as noted in table (4).

IX. INTERNAL FRICTION

Solid objects have a characteristic of mechanical resonant frequencies (f) which are related to the ribbons mass, dimension, and elastic properties. The vibration can be analyzed from the internal friction $\left(Q^{-1}\right)$point of view(r), i.e., the dissipation of vibration energy in the ribbon sample, or damping mechanical loss. Q^{-1} Can be deduced from the amplitude decay a free vibration. In general, the hysteretic rearrangement of microstructural features upon application of a dynamic load causes internal friction. It is noted from table (5)

System	Q^{-1}
Sn	0.057
Sn10Bi	0.006
Sn20Bi	0.009
Sn10Bi10	0.011
Sn20Bi20	0.004

Table (5)

That pure Sn, Sn10Bi, Sn20Bi, Sn10Bi20In melt-spun solder except Sn20Bi20In have a high Q^{-1}. The Q^{-1} values are large enough to neglect the contribution of the energy loses in the support Q^{-1} for Sn melt-Spun falls within the expected range[18].The large agglomeration of indium particles is thermally activated, which explains the sudden decrease in internal friction, Q^{-1} particularly in the case of Sn20Bi20In.One notices that the increase in indium content is out of favor.

System	H_v(Mpa)
Sn	55.898
Sn10Bi	242.233
Sn20Bi	257.434
Sn10Bi10In	250.079
Sn20Bi20In	191.237

Table (6)

X. Hardness measurement

The average hardness values indicated table (6),H_v increase slightly with the addition of the indium content, indicating that the bonding of the force between tin and bismuth is much stronger than that between tin and indium. Further, one can notice the average hardness value is lowest for the alloy Sn20Bi20In indicating that the bonding force between In and Sn or Bi decrease may also be related to a greater ease of compacting atoms to a more dense configuration

XI. CONCLUSION

In conclusion, we have succeeded in producing sample of Sn-Bi-In by a rapid solidification processing, in which tin-bismuth-indium melt-spun alloy containing two phases distributed uniformly with the Sn-matrix. The effect of In-content on the solidification behavior of SnBi melt-spun alloys have been investigated. It has been established that Sn-Bi-In ternary melt-spun ribbons with uniform structure can be produced by rapid solidification from melt using melt-spinning technique. In melt-spun ribbons, tin was dispersed uniformly as fine discrete crystals, tin complex-regular cell, and interemtallic compound cells were abscent. On the basis of our experiment results, we prefer Sn1oBi10In solder as obtained for intermediate. Step soldering in hermetic Packaging [5]. Due to it has a suitable properties as indicated in the following table (7a,b).

System	E (GPa)	B (GPa)	G (GPa)	Cell volume(Å3)	H_v(Mpa)
Sn10Bi10In	38	37	14	146.438	257.434

Table (7) a

System	Electrical Conductivity $\sigma(\Omega m)^{-1}$	$D_{th}x10^{-8}\left(m^2.\sec^{-1}\right)$
Sn10Bi10In	0.0159	15.367

Table (7) b

XII.Future Work

Future work will analyze the effect of compositional melt-spun ribbons so that we can understand the mechanisms by which soldering behavior may be improved.

REFRENCES

[1] S. Sengupta, H. Soda, A. Mclean, " Microstructure and properties of a bismuth –indium- tin eutectic alloy", Journal of Materials Science vol. 37, no. 9, PP. 1747- 1758, 2002.

[2] Ren-Kae Shlue, Leu-Wen Tsay Chun – Lun, and Jia Lin Ou, "A study of Sn-Bi-Ag(In) lead free solders", Journal of Materials Science, vol. 38, no. 6, PP. 1269 - 1279, 2003.

[3] M. Kamal and T.El-Ashram, "Zero and negative coefficients of resistivity of rapidly" Journal of Materials Science, vol.19, no. 1, PP. 91-96, 2008.

[4] W. yoon and J.H. pere pezko," the effect of pressure on metastable phase formation in the undercooled Bi-Sn system", Journal of Materials Science, vol. 23, no. 12, PP. 4300- 4306, 1988.

[5] Sun-Kyoung Seo,Moon Gicho, Hyunck Mo lee, and Won Kyoung choi, "comparison of Sn2.8Ag20In and Sn10Bi10In solders for intermediate-step soldering," Journal of Electronic Materials, vol. 35, no.11, PP. 1975- 1981, 2006.

[6] Mustafa Kamal and Usama S.Mohammad, A Review: Chill Block Melt Spin Technique,theories & Applications Bentham eBooks, PP. 42-69, 2012.

[7] Y.A.Geller, A. G. Rakhshtadt, Science of Materials, Mir publishers, vol. 138, 1977.

[8] E. Schreiber, O. L. Anderson, and N. Soga, Elastic constants and their Measurement McGraw-Hill Book Company, Library of congress cataloging in publication Data, PP. 82-125, 1973.

[9] M.kamal, and E.S.Gouda, "Effect of Rapid Solidification on Structure and Properties of Some Lead-Free Solder Alloys", Materials and Manufacturing processes, vol. 21, no. 8, PP. 736-740, 2006.

[10] B. S. Berry, W. C. pritchett, "Some physical properties of two amorphous metallic alloys", J. Appl. phys. vol. 44, no. 7, PP. 3122- 3127, 1973.

[11] J. J Gilman, "Relationship between impact yield stress and indentation hardness ", J. Appl. phys, vol. 46, no. 4, PP. 1435- 1436, 1975.

[12] B.D. Cullity, Elements of x-ray Diffraction, Addison –wesley publishing company, INC, London, England printed in the united state of American, PP. 317, 1959.

[13] C. P. Chou L.A. Davis, and R. Hasegawa, "Elastic constants of Fe(Ni,Co)- B glasses ", J. Appl. Phys. vol. 50, no. 5 , PP. 3334- 4338 , 1979.

[14] S. Block, G. I. piermarini, R. G. Munro, and W. Wong-Ng, "The Bulk Modulus and young's modulus of the superconductor Ba2cu3yo7 "Advanced Ceramic Materials, vol. 2, no. 3B ,Special Issue, PP. 601,1987

[15] Mustafa Kamal, A.El-Bediwi, A.R. Lashin, A.H. El-zarka," Copper effects in mechanical properties of rapidly solidified Sn–Pb–Sb Babbitt bearing alloys", Materials Science and Engineering A, vol. 530, PP. 327-332, 2011 .

[16] M. Kamal, A. B. El-Bediwi, T.El-Ashram, M. E. Dorgham, "The Role of valence Electron Concentration on the structure and properties of Rapidly Solidified Sn-Ag Binary Alloys", Materials Science and Applications, vol.3, PP.179-184, 2012.

[17] ASTME 756-83, Am.Soc.Testing and Materials 1984

[18] Metals Handbook (ASM International, Vol.2, 1990.